PULLOUT TESTS USING STEEL GRID REINFORCEMENTS WITH LOW-QUALITY BACKFILL

by
Dennes T. Bergado, Kam-Hung Lo, Jin-Chun Chai,
Ramaiah Shivashankar, Marolo C. Alfaro
and Loren R. Anderson

Reprinted from
Journal of Geotechnical Engineering, ASCE
Vol. 118, No. 7, July 1992
pp. 1047-1063

Pullout Tests Using Steel Grid Reinforcements with Low-Quality Backfill

By Dennes T. Bergado,[1] Associate Member, ASCE, Kam-Hung Lo,[2] Jin-Chun Chai,[3] Ramaiah Shivashankar,[4] Marolo C. Alfaro,[5] and Loren R. Anderson,[6] Member, ASCE

Abstract: Both laboratory and field pullout tests are conducted using steel grid reinforcements with cohesive-frictional backfill soils. The laboratory pullout tests are performed using a large-scale pullout apparatus designed especially for this study. The field pullout tests are performed on the dummy welded-wire reinforcements embedded in a full-scale reinforced test wall/embankment system that utilize three different locally available, low-quality, cohesive-frictional backfill soils, namely, clayey sand, lateritic soil, and weathered clay, in the three sections along its length. It is observed that the magnitudes of the mobilized field pullout resistances as well as the strains induced in the reinforcing elements are strongly influenced by the response of the wall/embankment system to the subsoil movements and the resulting arching effects due to the presence of the inextensible reinforcements. Meanwhile, the laboratory pullout test results generally seem to provide a conservative approximation of the field pullout resistances of the grid reinforcements in cohesive-frictional backfills. Using the finite element method to model the laboratory pullout tests, the analytical results are observed to agree fairly well with the experimental results.

Introduction

A welded-wire reinforced wall/embankment system was built at the campus of the Asian Institute of Technology (AIT) using three locally available cohesive-frictional backfill soils to investigate its performance on soft clay foundations. The potential use of low-quality backfill materials in mechanically stabilized earth structures was also investigated. The backfill soils, namely, clayey sand, lateritic soil, and weathered clay, were placed in the three sections along the length of the wall/embankment system. Field pullout tests were conducted by Lo (1990) on the dummy grid reinforcements embedded at different elevations in the wall. This paper discusses the results of the field and the laboratory pullout tests and the numerical modeling of the laboratory pullout tests.

Theoretical Background

For the soil sliding directly over the grid reinforcement, the resistance is provided by the friction between the soil and the grid reinforcement, and

[1]Assoc. Prof., Geotech. and Transp. Engrg. (GTE) Div., Asian Inst. of Tech., P.O. Box 2754, Bangkok, Thailand 10501.

[2]Geotech. Engr., Moh and Associates, Engrg. Consultants, (Hongkong), Ltd., 19th Floor, Loyong Court, 212-220 Lockart Rd., Wanchai, Hong Kong.

[3]Grad. Student, GTE Div., Asian Inst. of Tech., P.O. Box 2754, Bangkok, Thailand.

[4]Res. Assoc., Dept. of Civ. Engrg., Fac. of Sci. and Engrg., Saga Univ., 1 Honjo, Saga 840, Japan.

[5]Res. Assoc. GTE Div., Asian Inst. of Tech., P.O. Box 2754, Bangkok, Thailand.

[6]Prof., Coll. of Engrg., Utah State Univ., Logan, UT 84322-0500.

Note. Discussion open until December 1, 1992. To extend the closing date one month, a written request must be filed with the ASCE Manager of Journals. The manuscript for this paper was submitted for review and possible publication on November 28, 1990. This paper is part of the *Journal of Geotechnical Engineering*, Vol. 118, No. 7, July, 1992. ©ASCE, ISSN 0733-9410/92/0007-1047/$1.00 + $.15 per page. Paper No. 966.

the internal friction of the soil. But the pullout of the grid reinforcement is much more complex, and the total pullout resistance comprises two components, namely, the frictional resistance and the passive resistance. The magnitude of the frictional resistance, P_f, developed between the soil and the surface of the longitudinal bars, depends on the angle of the skin friction and the level of effective normal stress at the interface, as shown in (1) here.

$$P_f = A_s(\sigma'_a)(\tan \delta) \qquad (1)$$

where A_s = the surface area of the longitudinal bars; σ'_a = the average normal stress; and δ = the skin friction angle between the reinforcement and the soil. The passive resistance is due to the soil bearing on the transverse members of the grid. The mechanism is similar to that of the base pressures beneath a deep-seated foundation in soil (Jewell et al. 1984). For the passive resistance, Peterson and Anderson (1980) provided an expression that forms the upper-bound estimation, considering a normal characteristic field for a foundation rotated to the horizontal, as shown in Fig. 1(a). For this case:

$$\frac{\sigma'_b}{\sigma'_v} = \{\exp[\pi(\tan \phi')]\}\left[\tan^2\left(\frac{\pi}{4} + \frac{\phi'}{2}\right)\right] \qquad (2)$$

where σ'_b = the passive or the bearing resistance; σ'_v = the effective vertical stress; and ϕ' = the effective friction angle of the soil. Jewell et al. (1984)

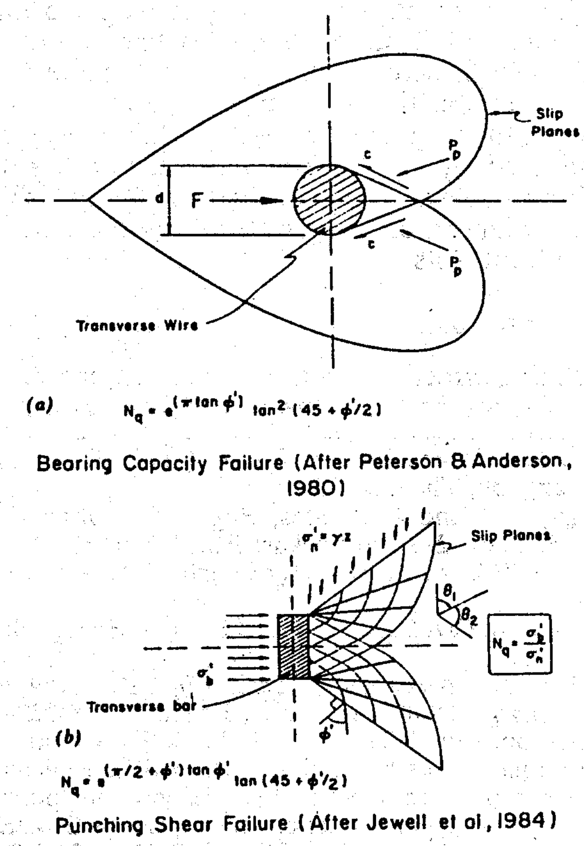

FIG. 1. Bearing Failure Mechanisms of Grid Reinforcement: (*a*) Shear Failure (Peterson and Anderson 1980); (*b*) Punching Failure (Jewell et al. 1984)

provided an expression that forms the lower-bound estimation, considering a punching failure model, as shown in Fig. 1(*b*). For this case:

$$\frac{\sigma'_b}{\sigma'_v} = \left\{\exp\left[\left(\frac{\pi}{2} + \phi'\right)(\tan\phi')\right]\right\}\left[\tan\left(\frac{\pi}{4} + \frac{\phi'}{2}\right)\right] \quad \ldots\ldots\ldots\ldots (3)$$

where all the terms are as defined previously.

In cases where cohesive or cohesive-frictional backfill soils are used, the short-term passive resistance can be predicted by (4) (Bergado et al. 1987).

$$\sigma_b = N_c C_u \quad \ldots\ldots\ldots\ldots (4)$$

where N_c = the bearing capacity factor for deeply embedded strip footing (Skempton 1951) taken as equal to 7.5 (Ingold 1983); and C_u = the undrained shear strength given as: $C_u = C + \sigma_n \tan\phi$, where C = the cohesion intercept, ϕ = the undrained frictional angle, and σ_n = the total normal stress. The total passive resistance, P_b, is expressed as follows:

$$P_b = A_b(n)(\sigma'_b) \quad \text{or} \quad P_b = A_b(n)(\sigma_b) \quad \ldots\ldots\ldots\ldots (5)$$

where A_b = the area of the individual transverse member perpendicular to the direction of the pull; and n = the number of transverse members in the grid reinforcement.

The total pullout resistance, P_t, is expressed as follows:

$$P_t = P_f + P_b \quad \ldots\ldots\ldots\ldots (6)$$

The welded-wire mesh reinforcement mat can be considered as a relatively inextensible reinforcement (Nielsen and Anderson 1984). The total pullout resistance was found to be a function of: (1) The number of transverse wires embedded behind the failure plane; (2) the diameter of the transverse wires; (3) the overburden pressures; (4) the moisture-density conditions of the backfill; and (5) the number, diameter, and length of the longitudinal wires. The contribution from the frictional resistance has been generally found to be less than about 10% (Jewell et al. 1984). Chang et al. (1977) observed that the mesh reinforcements generated 5–6 times more pullout resistances than the longitudinal wires only of an equivalent area.

Mechanically Stabilized Earth (MSE) Test Embankment

A full-scale test reinforced wall/embankment system with welded-wire reinforcements was constructed inside the campus of the Asian Institute of Technology (AIT), located 42 km north of Bangkok. The subsoil profile at the site comprises a topmost 2.0-m thick layer of dark-brown weathered clay overlying a layer of blackish-gray, soft clay, which extends to a depth of about 7.5 m below the existing ground level. The soft-clay layer is underlain by a layer of stiff clay. The ground-water table fluctuates between 1.0 and 2.0 m below the ground surface. A typical subsoil profile together with the general subsoil properties are depicted in Fig. 2.

The welded-wire reinforcement mats used in the MSE embankment system consisted of W4.5 (diameter = 6.1 mm) × W3.5 (diameter = 5.4 mm) galvanized steel wire meshes with 0.15-m-×-0.23-m (6-in.-×-9-in.) grid openings. Each reinforcing mat was 2.44 m (8 ft) wide and 5.72 m (18 ft, 9 in.) long, including the bent-up portion of the facing. The yield strength of the welded-wire bar was about 670 MPa, which occurred at very low

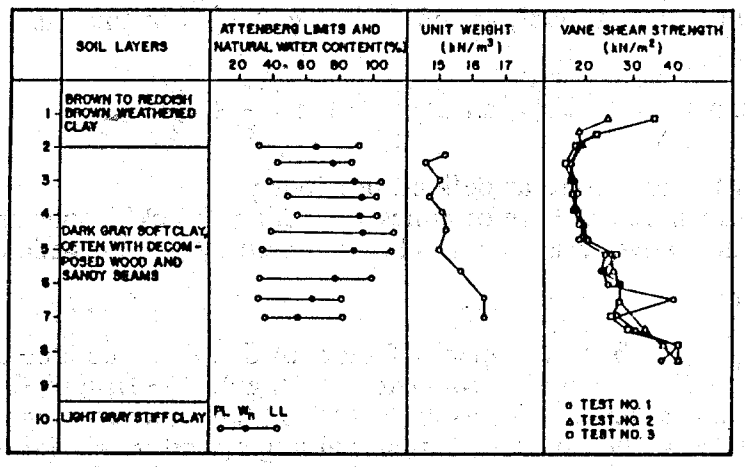

FIG. 2. Typical Subsoil Profile and Geotechnical Properties

strains in the order of about 0.4% to 0.5%, and the modulus of elasticity was approximately 183,145 MPa.

The construction guidelines set forth by the Hilfiker Company (*Welded* 1988) were followed. The construction took exactly a month between April 24 and May 24, 1989. The procedure involved the placement of the reinforcing mats with the bent-up portions forming the facing. Backing mats, screens, and easily compacted pea-size gravel were provided along the vertical face to prevent the erosion of the backfill soils. The backfill materials were then placed in three equal lifts between the two successive reinforcing layers, and each lift was compacted with a combination of a vibratory roller and a hand compactor to densities of about 95% of the standard Proctor on the dry side of the optimum moisture content. The basic properties of the backfill soils used in the three sections are shown in Table 1 (Bergado et al. 1989, 1990, 1991). Uniformity in compaction and moisture content during the construction was checked with a nuclear densitometer. The completed embankment was 5.70 m (18.7 ft) high. It has three sloping faces with 1:1 slopes and one vertical face (wall), as shown in Figs. 3(*a* and *b*).

The wall/embankment system was extensively instrumented for monitoring its performance. The instrumentation program included the measurement of the strains and, thereby, the tensions in the longitudinal wires. A total of seven mats were instrumented in each section. There were 12 instrumentation points on each of the bottom four instrumented mats and 10 instrumentation points on each of the top three instrumented mats. The axial strains were measured by using self-temperature compensating electrical resistant strain gages. At each instrumentation point, there were two strain gages placed diametrically opposite each other in order to cancel out the bending stresses. The surface and subsurface settlements, pore pressures, vertical pressures beneath the base of the wall, and lateral movements of the face of the wall and the subsoil were also monitored. Nine surface and 10 subsurface settlement plates were placed at different locations and at varying depths below the test embankment. Four pneumatic piezometers and six hydraulic piezometers were also installed. Of the five SINCO inclinometers, three were installed at the face, one at the center, and the other at the back. Two dummy reinforcement mats in each section intended for the field pullout tests were also instrumented with strain gages at selected

TABLE 1. Summary of Backfill Soil Properties

Soil (1)	G_s (2)	W_p (%) (3)	W_l (%) (4)	I_p (%) (5)	Passing sieve number 200 (0.075 mm) (%) (6)	W_{opt} (%) (7)	γ_{dmax} (kN/m³) (8)	Direct Shear		Unconsolidated Undrained		Isotropically Consolidated Undrained			
								C (kN/m²) (9)	ϕ (degrees) (10)	C (kN/m²) (11)	ϕ (degrees) (12)	$\bar{C}$ (kN/m²) (13)	$\bar{\phi}$ (degrees) (14)	C (kN/m²) (15)	ϕ (degrees) (16)
Clayey sand	2.55	—	—	—	44.28	14.0	17.0	38.0	26.8	42.0	23.5	25.0	24.0	32.0	18.2
Lateritic residual soil	2.61	23.20	39.20	16.00	17.91	11.5	19.3	88.0	40.2	80.0	32.5	27.0	25.2	30.0	21.0
Weathered clay	2.67	21.00	45.00	24.00	82.94	22.0	16.3	129.0	30.7	118.0	31.5	19.0	25.8	24.0	15.5

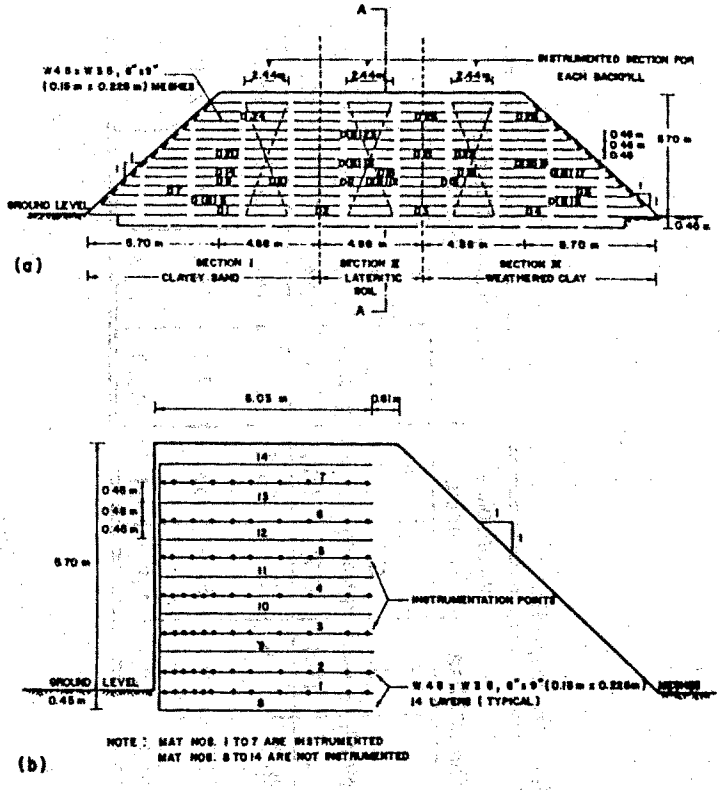

FIG. 3. Geometry of Reinforced Test Wall/Embankment: (*a*) Front View; (*b*) Sectional View

points and were embedded at different levels along the face of the wall. The locations of all the dummy mats are shown in Fig. 3(*a*).

FIELD PULLOUT RESISTANCES AND PREDICTIONS

A total of 15 constant-strain field pullout tests were conducted on the dummy reinforcement mats with varying overburden pressures, bar sizes, and mesh geometries. Three of these dummy mats had no transverse bars. They had only four longitudinal bars of size W4.5 (diameter = 6.1 mm) with short transverse ribs on them. The rest of the dummy mats had 0.15-m-×-0.23-m (6-in.-×-9-in.) grid openings, with 5 to 6 transverse bars. The average length of embedment of all the dummy mats was around 2.0 m behind the face of the wall. The geometry of the instrumented dummy mats together with the locations of the strain gages are shown in Fig. 4.

The pullout force was applied by an electrohydraulic servo-controlled cylinder through a steel reaction frame butting against the wall face. The horizontal displacements of the mats were monitored by using linear variable differential transformers (LVDTs) and dial gauges. A data-acquisition system consisting of a 21X micrologger with multiplexer and a storage module was employed to record the displacements of the mat, pullout forces, and the axial strains in the bars. The setup of field pullout test equipment is shown in Fig. 5. A constant pullout rate of 1.0 mm/min was adopted. All the mats were pulled out to a total displacement of about 130 mm (5 in.). The loads were measured with a 222.50-kN (50,000-lbs, 22.5-metric tons) capacity load cell.

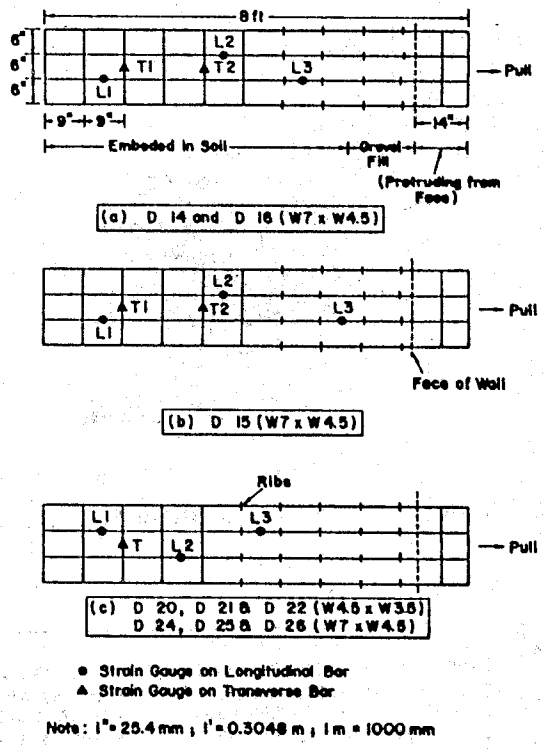

FIG. 4. Schematic Diagram of Dummy Mats Showing Locations of Instrumentation Points

The typical pullout force-mat displacement curves for the weathered clay backfill are shown in Fig. 6. All of the curves generally show a yield point, wherein there is a significant increase in displacements with only a small increase in the pullout force. However, there seems to be no well-defined peak in these load-displacement curves. The pullout force was still increasing at the end of 130-mm (5-in.) displacement. The pullout forces in such cases, however, were already near the tension capacity of the reinforcements. The results for the same size of bars, similar configuration of mat and overburden pressures for the three different types of backfill soils were compared as shown in Fig. 7. It can be seen that the pullout resistances of the dummy mats in clayey sand were higher.

From Fig. 6, it can be observed that the overburden pressures, bar sizes, and number of transverse bars definitely affected the total pullout resistances, conforming with the theoretical expectations. The pullout force increased almost linearly with the increase in the overburden pressures. On the contrary, in the case of the lateritic backfill soil there was a decrease in the maximum pullout resistances with the increase in the overburden pressures. The maximum pullout resistances of dummy mats D(B)23 and D(B)12 [see Fig. 3(*a*)] having similar bar sizes of W12 (diameter = 10 mm) × W5 (diameter = 6.4 mm) and almost the same length of embedment, but with varying overburden heights of 1.5 m and 3.8 m, respectively, demonstrate the contradiction. The maximum pullout resistance of the latter had reduced to about 50% of the former. This discrepancy can be attributed to the arching effects in the middle section of the wall/embankment system. At the wall facing, all the reinforcement layers were interconnected to the full height and length of the wall, which prevented the immediate response to the

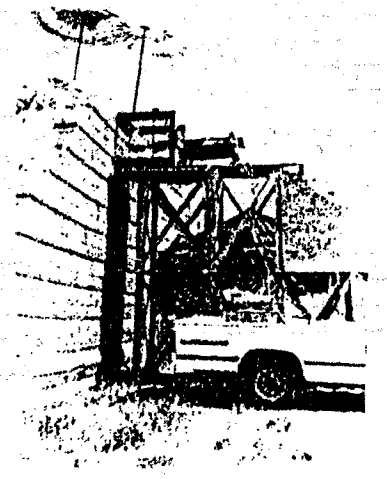

FIG. 5. Photograph Showing Setup of Field Pullout Test

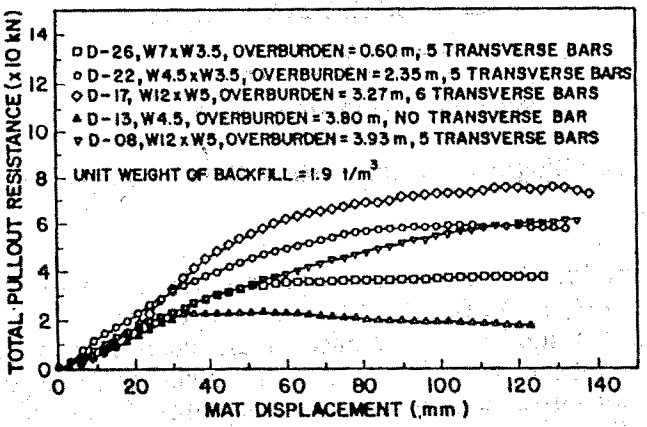

FIG. 6. Summary of Field Pullout Resistance versus Mat Displacement for Weathered Clay Backfill

settlements at the center, thereby causing arching effects beneath the vertical face. The arching effects must have influenced much the pullout resistances of the dummy mats, especially in the lower portions of the middle section (Bergado et al. 1991). Other factors, such as particle crushing of the lateritic soil and nonuniform moisture distribution within the reinforced mass also influenced the pullout resistances, although to a lesser extent.

The field pullout tests of the ribbed longitudinal bars (transverse bars being clipped) were conducted one in each of the three types of backfills, having the same overburden height of 3.8m. The pullout resistances obtained in the weathered clay and the clayey sand were slightly higher than that in the lateritic soil. It is possible that the resistance obtained in the lateritic soil would have been higher, but the arching effects must have drastically reduced the overburden pressures. The friction coefficient, f (assuming that the ribs contributed to an increase in the frictional resistance of the plain longitudinal bars), in each of the three types of backfill soil, was 2.77, 2.65, and 2.84 for clayey sand, lateritic soil, and weathered clay, respectively.

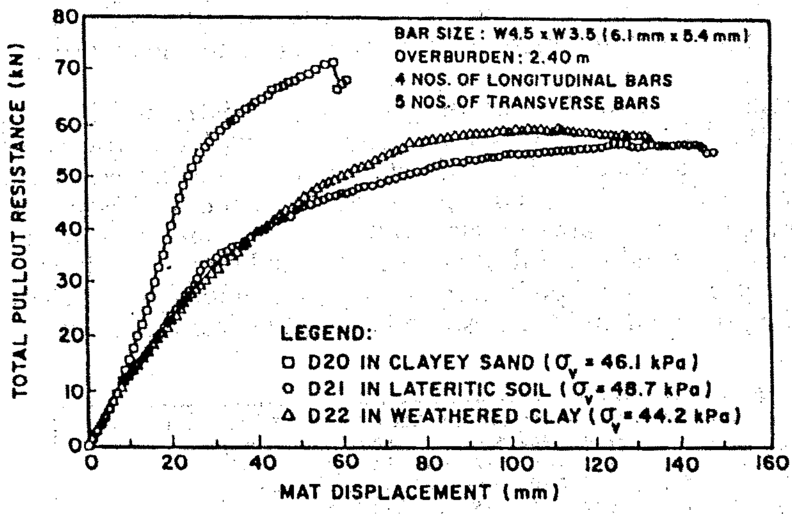

FIG. 7. Typical Plot of Field Pullout Resistances for Different Types of Backfills

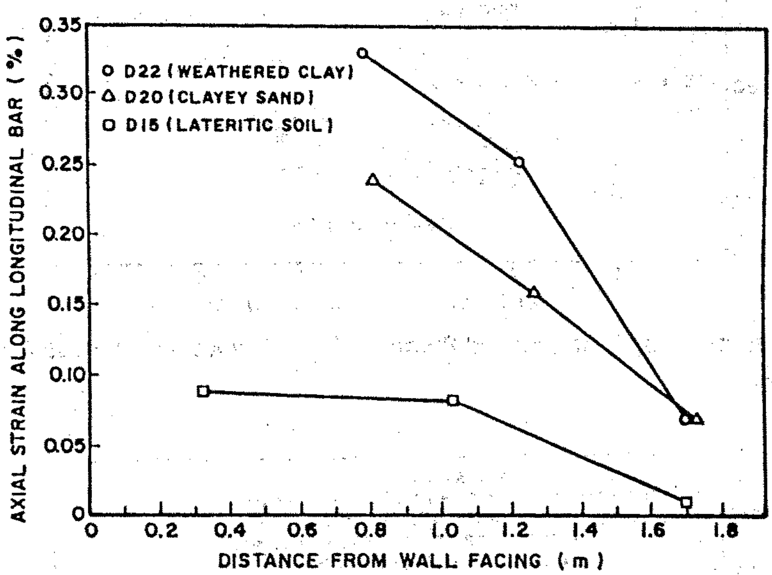

FIG. 8. Typical Plot of Axial Strains in Longitudinal Bar versus Distance from Wall Facing for Different Types of Backfill

For calculating the friction coefficient, f, the following equation was used (Nielsen and Anderson 1984):

$$f = \frac{P_f}{A_s(\sigma'_a)} \quad \text{.......} \quad (7)$$

where P_f = the peak pullout force of the ribbed longitudinal bars; A_s = the surface area of the longitudinal bars; σ'_a = the average overburden pressure; and $\sigma'_a = 0.75\sigma'_v$ (σ'_v being the vertical overburden pressure).

The plots of the strains in the dummy reinforcements during pullout tests with the distance from the facing are presented in Fig. 8. The results show that the axial strains in the longitudinal bars tend to decrease almost linearly with the increase in the distance from the face of the wall. The higher strains

measured in the clayey sand backfills and the weathered clay reflect the higher mobilized pullout resistances as compared to the lateritic backfill soil.

Predictions by the method of Bergado et al. (1987) and Peterson and Anderson (1980) [(1), (2), and (4)] were compared with the observed pullout resistances in Figs. 9 and 10 for the clayey sand and the weathered clay backfills, respectively. The predicted values of the pullout resistances were comparably good for weathered clay, but they were underestimated in the case of the clayey sand backfill. It should be noted that the influence of the arching effects on the field pullout resistances had made a direct comparison between the predicted and the observed pullout resistances rather difficult.

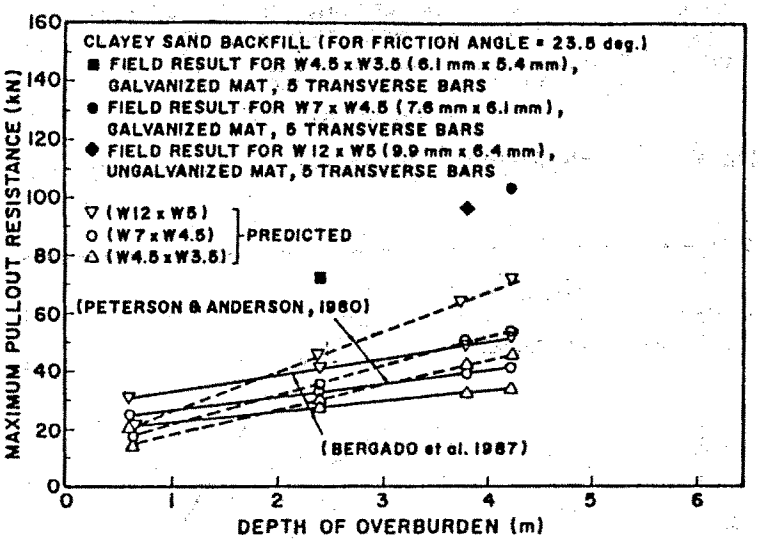

FIG. 9. Comparison of Observed and Predicted Field Pullout Resistances for Clayey Sand Backfill

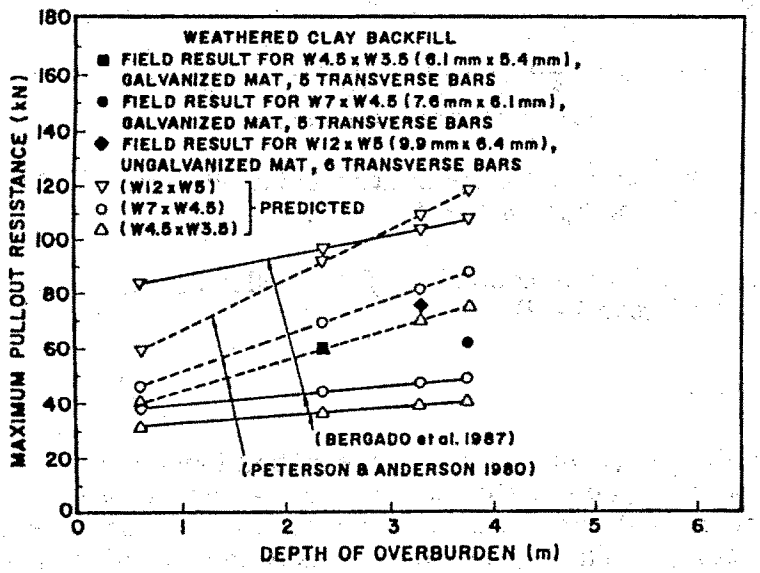

FIG. 10. Comparison of Observed and Predicted Field Pullout Resistances for Weathered Clay Backfill

Comparison of Laboratory and Field Pullout Resistances

The pullout box used in the laboratory pullout tests was built of 13-mm (1/2-in.) thick steel plates, rolled steel beams, and bolted connections with dimensions of 1.30 m × 0.80 m × 0.50 m (50 in. × 30 in. × 20 in.). The details of the laboratory pullout test setup, procedures, and preliminary results have been published elsewhere (Bergado et al. 1989; Cisneros (1989; Amin 1989; Hardiyatimo 1990; Macatol 1990).

The reinforcement mats used in both the laboratory and the field pullout tests had 0.15-m-×-0.23-m (6-in.-×-9-in.) grid openings with varied bar diameters, and most of them had five transverse bars. The length of embedments of the reinforcement mats in the laboratory pullout tests was about 1.0 m, while the length of embedments of the dummy reinforcement mats in the field pullout tests was around 2.0 m. In the case of the dummy mats, a regular 0.15-m-×-0.23-m (6-in.-×-9-in.) mat, about 2.0 m long, was used with some of the transverse bars clipped, with only five or six transverse members left.

In order to compare the field and the laboratory pullout resistances, two assumptions have been made: (1) The frictional and the passive resistances vary linearly with the surface area of the longitudinal members and the bearing area of the transverse members, respectively; and (2) constant values of the apparent friction coefficients between the ribbed longitudinal bars and the soils were assumed. The values of the apparent friction coefficients were taken as 2.77, 2.65, and 2.84 for clayey sand, lateritic soil, and weathered clay, respectively, as estimated from (7), based from the pullout tests results. The frictional resistances of the ribbed longitudinal bars were then calculated, utilizing the constant values of the apparent friction coefficients for each of the corresponding backfill soils.

Based on the assumptions, the field pullout resistances were corrected to be comparable with the laboratory results. Figs. 11–13 show the comparison between the field and the laboratory pullout capacities plotted against the vertical normal pressures. For the weathered clay and the clayey sand backfills, it was observed that the field pullout tests provided higher pullout capacities in all the cases. The arching effects of the embankment must have increased the vertical stresses on the two end sections comprised of the clayey sand and the weathered clay backfills. This phenomenon resulted in increased pullout capacities at the end sections. For the lateritic backfill soil in the middle section, however, the field pullout resistances were very much affected by the arching effects. At the 2.4-m overburden condition, the field test gave nearly the same pullout capacity as the laboratory tests at the corresponding normal stress. However, at the 3.33-m overburden condition, the field test provided much lower pullout resistance than that of the laboratory tests. These results indicate that the arching effects were dominant at the lower portions of the wall. It must be noted that the results of the laboratory pullout tests for lateritic soil could be fitted by a bilinear curve. This was attributed to the particle-crushing phenomenon of the lateritic soils at higher stresses.

During the laboratory tests, the interaction between the soil-reinforcement system and the rigid boundaries of the laboratory pullout box (especially the front face) in the small-scale tests can affect the generated pullout resistances. As the reinforcement is being pulled out from the box, lateral pressures may develop against the rigid front face, leading to the arching of the soil over the inclusion, which reduces the local vertical normal stresses on the reinforcements and, consequently, decreases the pullout

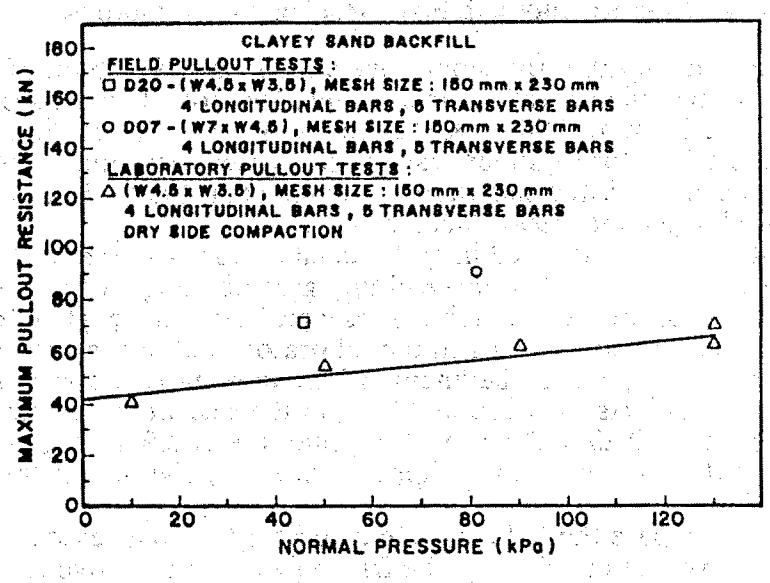

FIG. 11. Comparison of Field and Laboratory Pullout Resistances for Clayey Sand Backfill

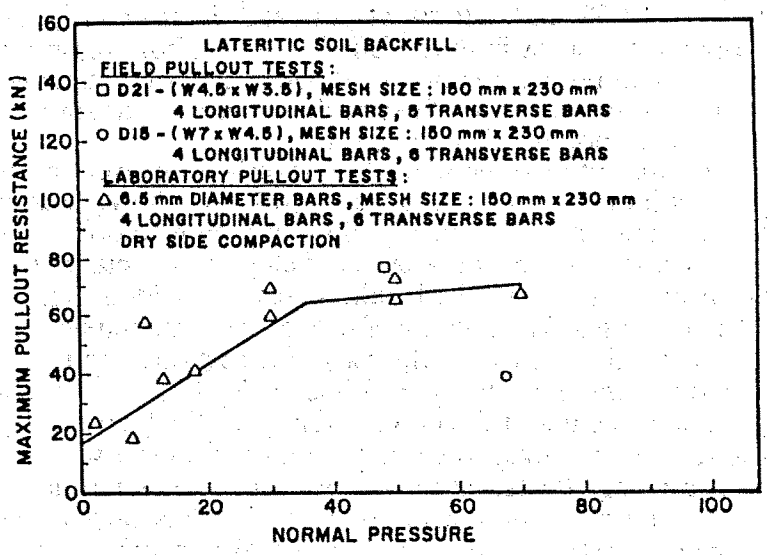

FIG. 12. Comparison of Field and Laboratory Pullout Resistances for Lateritic Soil Backfill

resistances (Juran et al. 1988; Palmiera and Milligan 1989). Dilatancy of soil during pullout tends to cause a localized increase in normal stresses acting on the reinforcements. Variation of the moisture content can also influence the friction between the soil and the reinforcement.

Numerical Modeling

Numerical modeling can be used to simulate the soil-reinforcement interaction during the pullout and also to simulate the behavior of the MSE structure to predict its performance. In this study, a computer program,

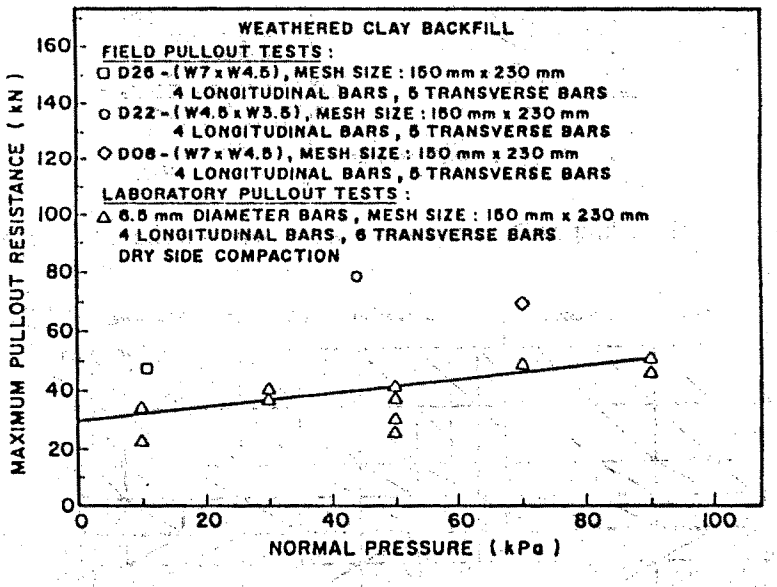

FIG. 13. Comparison of Field and Laboratory Pullout Resistances for Weathered Clay Backfill

TABLE 2. Soil Parameters Used in Finite Element Analysis

Soil type (1)	Parameters: Unit weight γ (kN/m³) (2)	k_0 value (3)	Cohesion C (kN/m²) (4)	Friction angle ϕ (degree) (5)	Modulus number k (6)	Modulus exponent n (7)	Failure ratio R_f (8)	Poisson's ratio ν (9)
Clayey sand	19.2	0.59	42.0	23.5	360	0.31	0.96	0.36
Lateritic soil	20.3	0.57	80.0	32.5	1400	0.34	0.96	0.36
Weathered clay	18.8	0.56	118.0	31.5	630	0.15	0.84	0.36

NONLIN 1, was modified and used to model the soil-reinforcement interaction during a laboratory pullout test. NONLIN 1 is a two-dimensional program that uses the initial stress method (Zienkiewicz et al. 1969) to represent the nonlinear behavior of the soil. The program is based on an analytical method suggested by Ochiai and Sakai (1987). The soil was represented by triangular and quadrilateral elements with a nonlinear elastic model criterion (Duncan and Chang 1970). The soil parameters used in the numerical modeling are given in Table 2.

The interface properties between the soil and the reinforcement were modeled by one-dimensional joint elements, and the relative displacement between the soil and the reinforcement was allowed if the mobilized shear stress at the interface equalled or exceeded the shear strength at the interface. This shear strength at the interface was obtained from Mohr-Coulomb strength theory. The parameters C and ϕ of the interface were set to be the same as those of the surrounding soil.

The reinforcement was represented by one-dimensional bar elements.

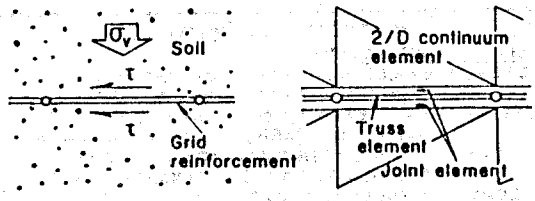

FIG. 14. Modelling of Reinforcement and Reinforcement-Soil Interface

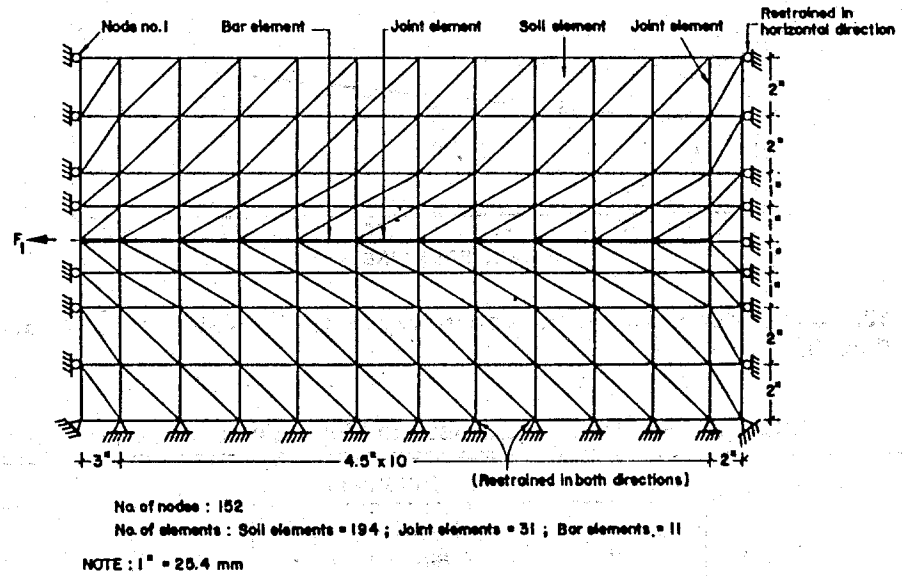

FIG. 15. Typical Finite Element Mesh for Analysis of Laboratory Pullout Test

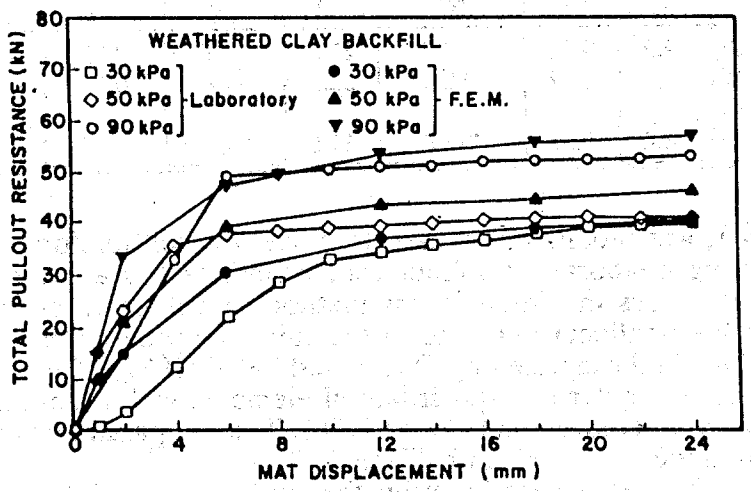

FIG. 16. Comparison of Experimental and Predicted Finite Element Method Load-Displacement Curves for Weathered Clay Backfill

The three-dimensional discrete bar mats were converted into two-dimensional representation (Schmertmann et al. 1989). The modulus of elasticity and the yield stress of the steel grids were set equal to the known standard values for steel. Fig. 14 shows the finite elements for the reinforcement and

the reinforcement-soil interface. A typical finite element mesh used for analyzing the laboratory pullout tests is shown in Fig. 15.

In order to define completely the load-displacement response during a pullout test, five displacement increments were considered. The displacements were specified to the nodal point at the free end of the reinforcement, just outside the front face of the pullout box. The comparison between the predicted load-displacement curves and those obtained from the actual laboratory pullout tests for 0.15-m-×-0.23-m (6-in.-×-9-in.) steel mesh with 6.5-mm (1/4-in.) diameter steel bars on weathered clay backfill are presented in Fig. 16. The predictions from the finite element analyses are comparable with the experimental results for all three types of backfill, with a maximum difference of about 15%, in terms of the pullout force.

Conclusions

Based on the results presented and discussed in this paper, the following conclusions can be drawn:

1. The pullout tests of the dummy mats in the two end sections of the wall/embankment system comprising the weathered clay and the clayey sand backfill soils proved that even with low-quality cohesive-frictional backfills, the pullout resistances increase with the increase in the overburden pressures.
2. The lateritic backfill soil in the middle section was very much affected by the arching effects and, therefore, yielded lower pullout capacities than the clayey sand or the weathered clay backfill soils. The clayey sand backfill was found to give higher pullout capacities than the weathered clay backfill.
3. The magnitudes of the mobilized pullout resistances as well as the strains in the reinforcing mats were found to be strongly influenced by the interacting performance of the embankment on soft clay foundation and the resulting arching effects due to the presence of the inextensible reinforcements.
4. Axial strains induced in the longitudinal bars were found to decrease lincarly with the increasing distance from the face of the wall.
5. The field pullout tests generally gave higher pullout capacities than the laboratory pullout tests, except for the middle section with lateritic backfill soil, especially in the lower portions, due to arching effects.
6. The predictions of Bergado et al. (1987) and Peterson and Anderson (1989) [i.e., (1), (2), and (4)] yielded values close to the observed field pullout capacities for the weathered clay backfill, but underestimated the pullout capacities in the case of the clayey sand backfill.
7. Using the modified finite element program NONLIN 1 to model the laboratory pullout tests, the load-displacement curves and the pullout capacities could be predicted comparably well with the experimental results.

Acknowledgments

This work was done as a part of a research project sponsored by the U.S. Agency for International Development (USAID), Bangkok, Thailand, conducted at the Asian Institute of Technology (AIT). The financial support provided by the USAID, Bangkok, Thailand and the facilities provided by AIT are gratefully acknowledged. The donations of steel grids by Hilfiker Company, Eureka, California is highly appreciated.

APPENDIX I. REFERENCES

Amin, N. U. (1989). "Direct shear and pullout tests on lateritic soil at low pressure," M Eng thesis, Asian Inst. of Tech., Bangkok, Thailand.

Bergado, D. T., Bukkanasuta, A., and Balasubramaniam, A. S. (1987). "Laboratory pullout tests using bamboo and polymer geogrids including a case study." Geotext. Geomembr., 5(3), 153–189.

Bergado, D. T., Cisneros, C. B., Sampaco, C. L., Shivashankar, R., and Alfaro, M. C. (1989). "Pullout resistance of steel grids with weathered clay backfill." *Proc. Symp. on Application of Geosynthetic and Geofiber in Southeast Asia*, Institution of Engineers, 1–26 to 1–33.

Bergado, D. T., Sampaco, C. L., Shivashankar, R., Alfaro, M. C., Anderson, L. R., and Balasubramaniam, A. S. (1990). "Interaction of welded wire reinforcement with poor quality backfill." *Proc. 10th Southeast Asian Geotech. Conf.*, Chinese Institute of Civil and Hydraulic Engineering, 1, 29–34.

Bergado, D. T., Sampaco, C. L., Shivashankar, R., Alfaro, M. C., Anderson, L. R., and Balasubramaniam, A. S. (1991). "Performance of welded wire wall with poor quality backfills on soft clay." *ASCE Geotech. Engrg. Congress*, ASCE, New York, N.Y.

Chang, J. C., Hannon, J. B., and Forsyth, R. A. (1977). "Pullout resistance and interaction of earthwork reinforcement and soil." *Transp. Res. Record 640*, 1–7.

Cisneros, C. B. (1989). "Pullout resistance of steel grids with weathered clay as backfill materials," M Eng. thesis, Asian Inst. of Tech., Bangkok, Thailand.

Duncan, J. M., and Chang, C. Y. (1970). "Nonlinear analysis of stress and strain in soils." *J. Soil Mech. Found. Div.*, ASCE, 96(5), 1629–1653.

Hardiyatimo, H. C. (1990). "Behavior of mechanically stabilized embankment on soft Bangkok clay," M Eng. thesis, Asian Inst. of Tech., Bangkok, Thailand.

Ingold, T. S. (1983). "Laboratory pullout testing of grid reinforcement in clay." *Geotech. Test. J*, 6(3), 112–119.

Jewell, R. A., Milligan, G. W. E., Sarsby, R. W., and Dubois, D. (1984). "Interaction between soil and geogrids." *Proc. of the Symp. on Polymer Reinforcement in Civil Engrg.*, Thomas Telford Ltd., London, U.K., 19–29.

Juran, I., Knochenmos, G., Acar, Y. B., and Arman, A. (1988). "Pullout response of geotextiles and geogrids (synthesis of available experimental data)." *Geosynthetics for soil improvements*, R. D. Holtz, ed., ASCE, New York, N.Y., 92–111.

Lo, K. H. (1990). "Modeling of laboratory and field pullout test of steel geogrid reinforcement," M Eng. thesis, Asian Inst. of Tech., Bangkok, Thailand.

Macatol, K. C. B. (1990). "Interaction of laterite backfill and steel grid reinforcements at high vertical stress using pullout tests," M Eng. thesis, Asian Inst. of Tech., Bangkok, Thailand.

Nielsen, M. R., and Anderson, L. R. (1984). *Pullout resistance of wire mats embedded in soil*. Utah State Univ., Logan, Utah.

Ochiai, H., and Sakai, A. (1987). "Analytical method for geogrid reinforced soil structures." *Proc. of the Int. Symp. on Geosynthetics*, Japanese Chapter of International Geotechnical Society, 483–486.

Palmiera, E. M., and Milligan, G. W. E. (1989). "Scale and other factors affecting the results of pullout tests of grids buried in sand." *Geotechnique*, 39(3), 515–524.

Peterson, L. M., and Anderson, L. R. (1980). "Pullout resistance of welded wire mats embedded in soil," M Sci. thesis, Utah State Univ., Logan, Utah.

Schmertmann, G. R., Chew, S. H., and Mitchell, J. K. (1989). "Finite element modelling of reinforced soil wall behavior." *Geotech. Engrg. Report UCB/GT/89-01*, Univ. of California, Berkeley, Calif.

Skempton, A. W. (1951). "The bearing capacity of clay." *Proc. Building Research Congress*, England, 1.

Welded wire wall construction guide. (1988). Hilfiker-Texas Corp., Eureka, Calif.

Zienkiewicz, O. C., Valliappan, A., and King, O. P. (1969). "Elastoplastic solutions of engineering problems: Initial stress, finite element approach." *Int. J. Numer. Methods Engrg.*, 1(1), 75–10.

APPENDIX II. NOTATION

The following symbols are used in this paper:

A_b = cross-sectional area perpendicular to direction of individual transverse member;
A_s = surface area longitudinal bars;
C = cohesion intercept;
C_u = undrained shear strength;
f = friction coefficient;
N_c, N_q = bearing-capacity factors;
n = number of transverse members of grid reinforcement;
P_b = total passive resistance;
P_f = total frictional resistance;
P_t = total pullout resistance;
δ = frictional angle between reinforcement and soil;
σ'_a = effective overburden pressure;
σ_b = soil short-term passive bearing capacity of cohesive or cohesive-frictional backfill;
σ'_b = soil passive bearing capacity;
σ_n = total normal stress;
σ_v = effective vertical stress;
ϕ = undrained frictional angle of soil; and
ϕ' = effective frictional angle of soil.